HHS Public Access

Author manuscript

Nat Genet. Author manuscript; available in PMC 2009 December 01.

Published in final edited form as:

Nat Genet. 2009 June ; 41(6): 739–745. doi:10.1038/ng.366.

A common allele in *RPGRIP1L* is a modifier of retinal degeneration in ciliopathies

Hemant Khanna[1,19], **Erica E. Davis**[2,19], **Carlos A. Murga-Zamalloa**[1], **Alejandro Estrada**[1], **Irma Lopez**[3], **Anneke I. den Hollander**[4], **Marijke N. Zonneveld**[4], **Mohammad I. Othman**[1], **Naushin Waseem**[5], **Christina F. Chakarova**[5], **Cecilia Maubaret**[5], **Anna Diaz-Font**[6], **Ian MacDonald**[7], **Donna M. Muzny**[8], **David A. Wheeler**[8], **Margaret Morgan**[8], **Lora R. Lewis**[8], **Clare V. Logan**[9], **Perciliz L. Tan**[2], **Michael A. Beer**[2,10], **Chris F. Inglehearn**[9], **Richard A. Lewis**[11], **Samuel G. Jacobson**[12], **Carsten Bergmann**[13], **Philip L. Beales**[6], **Tania Attié-Bitach**[14], **Colin A. Johnson**[9], **Edgar A. Otto**[15], **Shomi S. Bhattacharya**[5], **Friedhelm Hildebrandt**[15,16], **Richard A. Gibbs**[8], **Robert K. Koenekoop**[3], **Anand Swaroop**[1,15,17], and **Nicholas Katsanis**[2,18]

[1]Department of Ophthalmology and Visual Sciences, University of Michigan, Ann Arbor, Michigan 48105, USA. [2]McKusick-Nathans Institute of Genetic Medicine, Johns Hopkins University School of Medicine, Baltimore, Maryland 21205, USA. [3]McGill Ocular Genetics Laboratory, McGill University Health Centre, Montreal, Quebec, Canada. [4]Department of Human Genetics, Nijmegen Centre for Molecular Life Sciences, Radboud University Nijmegen Medical Centre, Nijmegen, The Netherlands. [5]Institute of Ophthalmology, UCL, London, UK. [6]Molecular Medicine Unit, Institute of Child Health, University College London, London WC1N 1EH, UK [7]Ophthalmic Genetics and Visual Function Branch, National Eye Institute, Bethesda, MD, USA. [8]Human Genome Sequencing Center, Baylor College of Medicine, Houston, Texas 77030, USA. [9]Section of Ophthalmology and Neurosciences, Leeds Institute of Molecular Medicine, St. James's University Hospital, Leeds, United Kingdom. [10]Department of Biomedical Engineering, Johns Hopkins University School of Medicine, Baltimore, Maryland 21205, USA. [11]Departments of Ophthalmology, Molecular and Human Genetics, Pediatrics, and Medicine, Baylor College of Medicine, Houston, Texas 77030, USA. [12]Scheie Eye Institute, Department of Ophthalmology, School of Medicine, University of Pennsylvania, Philadelphia, PA 19104, USA. [13]Department of Human Genetics, RWTH University of Aachen, 52074 Aachen, Germany [14]Département de Génétique et INSERM U-781, Hôpital Necker-Enfants Malades, Paris Cedex 15, France. [15]Department of Human Genetics, University of Michigan, Ann Arbor, Michigan 48105, USA. [16]Howard Hughes Medical Institute and Department of Pediatrics, University of Michigan, Ann Arbor, Michigan, 48105 [17]Neurobiology Neurodegeneration & Repair Laboratory, National Eye Institute, Bethesda, Maryland, USA. [18]Wilmer Eye Institute and Department of Molecular Biology and Genetics, Johns Hopkins University School of Medicine, Baltimore Maryland 21205, USA

Abstract

Correspondence to: AS[1,15,17] e-mail: swaroopa@nei.nih.gov and NK[2,18] e-mail: katsanis@jhmi.edu.

[19]These authors contributed equally to this work.

Despite rapid advances in disease gene identification, the predictive power of the genotype remains limited, in part due to poorly understood effects of second-site modifiers. Here we demonstrate that a polymorphic coding variant of *RPGRIP1L* (retinitis pigmentosa GTPase regulator-interacting protein-1 like), a ciliary gene mutated in Meckel-Gruber (MKS) and Joubert (JBTS) syndromes, is associated with the development of retinal degeneration in patients with ciliopathies caused by mutations in other genes. As part of our resequencing efforts of the ciliary proteome, we identified several putative loss of function *RPGRIP1L* mutations, including one common variant, A229T. Multiple genetic lines of evidence showed this allele to be associated with photoreceptor loss in ciliopathies. Moreover, we show that RPGRIP1L interacts biochemically with RPGR, loss of which causes retinal degeneration, and that the 229T-encoded protein significantly compromises this interaction. Our data represent an example of modification of a discrete phenotype of syndromic disease and highlight the importance of a multifaceted approach for the discovery of modifier alleles of intermediate frequency and effect.

The ciliopathies are a collection of disorders with overlapping clinical manifestations that include renal cystic disease, polydactyly, retinal degeneration and defects of the central nervous system1, and provide a useful model to investigate both the effects of variation at a single locus and the potential epistatic interactions between alleles at functionally related loci. This is because several ciliopathy-causing genes can either cause a distinct recessive form of ciliary disease or contribute modulators of penetrance and expressivity. In some instances, multiple allelism at a single locus can partially explain phenotypic variability. For example, null mutations in *NPHP3* cause MKS2, while hypomorphic *NPHP3* alleles cause Nephronophthisis (NPHP)3. Similarly, hypomorphic *CEP290/NPHP6* mutations are observed frequently in Leber congenital amaurosis (LCA) in both humans and in a mouse model4,5, whereas loss-of-function mutations lead to a constellation of ciliopathies that include MKS, NPHP, Bardet-Biedl Syndrome (BBS) and JBTS6-9 without a clear explanation for the phenotypic variation.

Consistent with the suggestion of second-site modifiers, several alleles are reported to modify ciliary phenotypes; a hypomorphic mutation in *MGC1203* contributes to the overall penetrance and expressivity of BBS10, while heterozygous variants in *CEP290* and *AHI1* contribute to the phenotypic severity and pleiotropy of NPHP11. Finally, likely additive effects between alleles in *bona fide* BBS and MKS loci produce hybrid phenotypes of the two clinical entities7.

A paradigm emerging from the above studies is that genes mutated in one ciliopathy may contribute alleles across the entire clinical spectrum and that the assessment of total mutational load across the ciliary proteome12,13 will help dissect phenotypic causality and variability. Towards this end, we have initiated two complementary strategies – interactome studies on ciliary proteins and medical resequencing of known ciliopathy genes across a cohort of patients with diverse phenotypes (MKS and JBTS as severe, BBS as intermediate, NPHP and LCA as mild).

We first investigated *RPGRIP1L*, under the hypothesis that in addition to its association with MKS and JBTS14,15, it might also contribute alleles to other ciliary disorders. We screened 166 unrelated patients of northern European descent (17 MKS, 15 NPHP (with and without

extra-renal phenotypes), 34 BBS, 100 LCA) and discovered 10 different novel nonsynonymous changes in 24 individuals (Table 1). We also detected two different common variants G1025S (rs2111119) and D1264N (rs3213758), both of which are present at similar allele frequencies when compared across our ciliopathy cohort, a cohort of 96 control individuals of northern European descent, and 60 CEPH controls from HapMap (data not shown).

None of the observed alleles are sufficient to explain disease manifestation under a Mendelian model. However, most alleles were either unique to our patient population, or were enriched compared to ethnically matched controls, and mapped within known functional domains of RPGRIP1L (Table 1; Suppl. Fig. 1).

However, the rarity of most alleles precluded us from delineating their impact on the clinical phenotypes. One notable exception, A229T, is sufficiently frequent to empower such a study. To assess allele neutrality without a preconceived model of inheritance, we performed Transmission Disequilibrium Testing (TDT); we screened 145 BBS families for which DNA was available from both parents. Focusing on families in which only one of the two parents was an A229T heterozygote, we identified 18 informative trios and detected significant over-transmission of the threonine-encoding allele in patients (15/18 transmissions; 83.3%, $p<0.01$).

Despite the modest number of trios, the TDT suggested that the A229T change is not neutral. To probe this possibility further, we re-evaluated our original resequencing data. We found a surprising enrichment of the 229T allele in northern European patients in whom retinal degeneration is mandatory for diagnosis, such as in BBS or Senior-Loken Syndrome (SLS) (5.9%; 4/68 chromosomes, and 15%; 3/20 chromosomes respectively; Table 1, compared to a 2.8% allele frequency in unaffected northern Europeans; Table 2). We therefore wondered whether this variant might contribute to the retinal defect, which is a frequent, but not ubiquitous, ciliopathy phenotype. If this is true, then comparisons between NPHP (no retinal degeneration) versus SLS cohorts (NPHP and retinal degeneration) should be informative. Even though each of these phenotypes is rare in the general population, we were able to study two northern European cohorts: 66 unrelated patients with isolated NPHP and 84 patients with SLS. Remarkably, 229T was absent from the NPHP group, but was detected at an allele frequency of 5.4% in SLS patients (Table 2). The small size of this cohort precluded meaningful statistical analysis. Nonetheless, these data suggested that the absence of 229T might have a protective effect from RP.

To investigate this possibility, we queried whether the 229T allele frequency is significantly different in a larger case-control cohort of northern European ciliopathy patients (Suppl. Table 1). We categorized our patients into two groups, with retinal phenotypes being the sole distinguishing factor. Both groups exhibited significantly different 229T allele frequencies compared to controls (n=3016 control alleles); the allele was absent from the non-retinal degeneration group (n=230 alleles; p=1.92E-03) but was enriched in the retinal degeneration group (combined: 4.5%, n=974 alleles, p=6.45E-03; Table 2). Furthermore, in agreement with our earlier data, we observed significantly different 229T allele frequencies between the non-retinal pathology and retinal degeneration ciliopathy groups (p=7.35E-05;

Table 2). To evaluate the statistical significance of our findings further, we performed permutation analyses where the observed genotypes in the entire sample were assigned randomly without replacement in the three groups (ciliopathy +RP, ciliopathy −RP, controls). After 10^7 independent random assignments, we counted the number of times that the differences in minor allele frequency in each group matched or exceeded the actual differences. This study provided additional evidence that the association data did not occur by chance (Table 2). Importantly, we found A229T to be transmitted through at least three different haplotypes (three patients contained unique *RPGRIP1L* SNPs *in cis* with 229T), while the frequency of 229T was indistinguishable across cohorts collected at different sites (Suppl. Table 1), arguing against a stratification artifact.

Our genetic data suggest a role for 229T in the development of RP in ciliopathy patients. However, the low frequency of this allele in the population and its apparent modest effect in our cohorts limit the power of genetic studies. We therefore evaluated the potential consequences of A229T to protein function.

As a first test, we performed a genetic rescue experiment using an *in vivo* model. We have shown previously that suppression of ciliary and basal body proteins in zebrafish leads to measurable phenotypes in mid-somitic embryos, some of which are caused by defects in Wnt signaling16,17, a phenotype also observed in other experimental ciliopathy models18. The ability of human mRNA to rescue somitic phenotypes has proven useful for establishing the pathogenic potential of alleles by comparing the efficiency of rescue of wild type (wt) human messenger RNA (mRNA) compared to mRNA bearing the missense variant(s) under investigation7. We identified a single partial zebrafish transcript that, upon reciprocal BLAST analysis, showed the highest amino acid similarity between zebrafish and human (73% similarity, 55% identity), to which we designed a splice-blocking morpholino (MO). The MO was injected into wild-type (wt) embryos at the two-cell stage (50-100 embryos per injection) and scored at the eight to nine somite stage. Consistent with data from other ciliopathy genes7,10,16,17, we observed dose-dependent gastrulation defects that included a shortened body axis, thin somites with broad lateral extensions, minor kinking of the notochord, underdeveloped anterior structures and tail extension abnormalities, all of which enabled us to categorize embryos into two classes based on objective criteria (Class I or Class II; Fig. 1a; Suppl. Fig. 2a). These phenotypes resulted from loss of *rpgrip1l*, since RT-PCR and sequencing analysis of embryos showed 10 ng of MO to cause ∼50% reduction of *rpgrip1l* mRNA (Suppl. Fig. 2b). Importantly, the phenotypes could be rescued by co-injection of 50 pg of wt human mRNA (embryos scored blind to injection cocktails; Fig. 1b, Suppl. Table 2).

We therefore proceeded to compare the efficiency of rescue between human mRNA encoding each of 229A and 229T. In addition, we included two known pathogenic missense alleles, T615P and A695P, that cause JBTS14,15 as positive controls, as well as the neutral G1025S variant as a negative control. Embryos were co-injected with a cocktail of MO and each human mRNA (n=88-115 embryos per allele) and scored blind to the injection cocktail (Suppl. Table 2). We found that the 229T rescue gastrulation phenotype was significantly different from wt mRNA rescue ($p<0.0001$; Fig1b, Suppl Table 2). The assay was specific, since each of T615P and A695P were scored as pathogenic, but had no off-target effects; the

rescue of the 1025S-encoding mRNA was indistinguishable from the 1025G message (Fig1b).

To substantiate these assessments, we measured embryonic structures labeled *in situ* with *pax2*, *krox20*, and *myoD* riboprobes. On whole embryo flat-mounts age-matched to eight to nine somites, we calculated the ratio of the width (w) spanning the distal ends of the 5th somites to the length (l) of the notochord as demarcated by adaxial cell labeling (n=8-20 embryos measured per variant). Consistent with our live embryo scoring, comparison of the mean w/l ratios between wt and mutant rescues indicated that both positive control alleles and A229T, but not G1025S, are pathogenic (Fig. 1c, d; Suppl. Table 3).

As a third line of *in vivo* evidence, we examined 5-day *rpgrip1l* morphant larvae (n=52-78 embryos/injection). Consistent with other ciliopathy morphants19, we observed tail extension abnormalities in 35% of *rpgrip1l* morphants, which was rescued by co-injection of wt human *RPGRIP1L* message (Fig. 1e, f). However, mRNA encoding 229T was unable to efficiently rescue the tail phenotype (p=0.031), consistent with both the T615P and A695P rescues (p=0.001 and 0.004 respectively). These observations, in addition to the absence of tail phenotypes in morphants rescued with G1025S mRNA, substantiated further the specificity of our assay (Fig. 1e, f).

We next turned to the question of why A229T might have the observed effect on the retinal degeneration phenotype. We noted that mutations in one of the NPHP genes, *NPHP5*, are also associated with an increased incidence of SLS; all tested patients with *NPHP5* null variants exhibit retinal degeneration compared to a 10% incidence of retinopathy in patients with mutations in other NPHP-associated genes20. NPHP5 interacts with RPGR20, a ciliary protein mutated in 70-80% of X-linked RP and 20-25% of simplex RP21-24. We therefore hypothesized that RPGRIP1L might also interact biochemically with RPGR and that the A229T allele might have a measurable effect on the affinity of this interaction. As part of our ongoing efforts to understand the pathobiology of RPGR, we had performed yeast two-hybrid (Y2H) screens of human retinal cDNA as prey using full-length RPGR^{ORF15} as bait and identified the carboxyl-terminal domain of RPGRIP1L (RPGR-interacting domain; RID); this interaction was validated by known-bait and known-prey analysis using different domains of RPGR as bait (Fig. 2a, b). To corroborate the findings, we generated an anti-human RPGRIP1L antibody (Suppl. Fig. 3) and performed co-immunoprecipitations (IP) using bovine retinal extracts. In reciprocal IP experiments with RPGRIP1L or RPGR antibody, we detected the expected bands on immunoblots corresponding to RPGR or RPGRIP1L, respectively (Fig. 2c). Co-transfection of COS-1 cells followed by co-IP demonstrated that Xpress-tagged RPGR and GFP-RPGRIP1L proteins are part of the same complex (Fig. 2d). We then tested A229T and three reported JBTS variants14,15 that are shown to be pathogenic in our zebrafish assay. Triplicate experiments showed that the GFP-tagged A229T mutant protein showed considerably lower (∼80%) ability to immunoprecipitate RPGR and has a profound effect on RPGR binding compared to the JBTS mutations (Fig. 2e, f). We also found that RPGRIP1L localizes to the cilium and basal body of mouse IMCD3 cells and to the inner segment/connecting cilium of mouse photoreceptors (Suppl. Fig. 4), in the same spatiotemporal context as demonstrated

previously for RPGR4,23,24. Hence, the abrogation of RPGRIP1L-RPGR interaction is likely to be relevant in photoreceptors.

Second-site modifications are emerging as prevalent phenomena in Mendelian disorders. For example, PLS3 is a protective modulator of SMN1 dysfunction associated with Spinal Muscular Atrophy (SMA)25; mutations in *CNTF* modify the age of onset in amyotrophic lateral sclerosis (ALS)26, while a mutation in *MGC1203* can modify the global penetrance/expressivity in BBS10. However, the penetrance and expressivity of tissue-specific defects within the context of syndromic disease pose a considerable challenge, especially for alleles of modest frequency in the general population and modest effect on the phenotype, which cannot be captured by traditional population-based genetic tools. Our data suggest that, in patients of northern European descent, the presence of the 229T allele of RPGRIP1L has predictive value for retinal degeneration. It will be important to consider the nature and position of mutations at the primary locus, since A229T probably exerts its effect in the context of mutations in specific ciliopathy proteins that can complex with RPGR in the retina; this is consistent with the previously proposed poison model of genetic epistasis27.

It is possible that some of the other alleles reported herein might also exhibit a similar effect; however, their rarity will necessitate the evaluation of larger cohorts. Notably, *in vivo* evaluation of each of the rare alleles using the zebrafish rescue assay suggested that most are pathogenic (Table 3, Suppl. Table 2, Suppl. Table 3, Suppl. Fig 5) and that they can potentially interact with alleles at various sites of the ciliopathy genetic spectrum (Table 1). Also, destabilization of the RPGRIP1L-RPGR complex is unlikely to be the sole cause of retinal degeneration. RPGRIP1L also associates with RPGRIP1 (Fig. 2c), null mutations in which cause early-onset, severe retinal degeneration28. Three of the alleles found in our cohort, A1183G, R1236C and D1264Y map within the RPGRIP1-interacting domain of RPGRIP1L; hence, their contribution to disease might be mediated by loss of RPGRIP1 activity/function. Finally, RPGRIP1L and RPGR are members of a larger macromolecular complex whose composition and function will vary across tissue types and ciliary functions. Establishment of the content and the stoichiometry of such complex(es), coupled to the evaluation of ciliopathy alleles on the stability of the macromolecular complex in a tissue/function-dependent manner will enable the currently poor allelic stratification of variability in disease phenotypes.

Methods

Ciliopathy patients, controls, and mutational analysis

Control DNAs were obtained from healthy individuals with no clinical ciliopathy criteria (retinal degeneration, polydactyly, renal abnormalities, mental retardation or other central nervous system defects) from four collection points (Suppl. Table 1). Blood samples were obtained following informed consent. We amplified the exon sequence and intron/exon junctions of *RPGRIP1L* (NM_015272) from DNA extracted from lymphoblast cell lines or lymphocytes according to standard protocols. PCR products were sequenced with BigDye Terminator v3.1 chemistry on an ABI 3100 or ABI 3730 (Applied Biosystems), sequences were analyzed with PolyPhred, and variants were confirmed by resequencing and visual

assessment of chromatograms. Primer sequences and PCR conditions are available upon request.

Statistical analyses

We used plink v1.04 (http://pngu.mgh.harvard.edu/purcell/plink/) for TDT analysis in BBS trios, and the PEPI404x package for Fisher's exact test. All other analyses were performed in Microsoft Excel.

DNA constructs

We generated full-length or specific domains of *RPGR* by PCR from retinal cDNA and subcloned them into the pcDNA 4 expression vector (Invitrogen). Full-length *RPGRIP1L* was amplified from human retinal cDNA, cloned into expression vector pEGFP-C1 (*in vitro* assays) or pCS2+ (*in vivo* assays) and confirmed by direct sequencing. Mutagenesis was performed using the QuickChange Site-Directed Mutagenesis kit (Stratagene), according to manufacturer's instructions.

Zebrafish embryo manipulation and morpholino injection

A splice-blocking MO (Gene Tools) was diluted to appropriate concentrations in deionized, sterile water (2, 4, 6, 8, and 10ng/nl for the dose response, and 10ng/nl for rescue experiments) and was injected into wt zebrafish embryos at the two-cell stage as described10. To rescue the MO phenotype, we transcribed mRNA from linearized pCS2+-*RPGRIP1L* vector with the SP6 mMessage machine kit (Ambion). We carried out *in situ* hybridization on whole embryos fixed with 4% paraformaldehyde with riboprobes against *pax2*, *krox20*, and *myoD* using standard protocols. Images were captured at 10X magnification and measurements were taken of the width spanning the 5^{th} somites from the anterior end, and the length of the notochord as defined by *myoD* staining of adaxial cells. Embryos used for assessment of tail phenotypes at 5dpf were reared in 1-phenyl-2-thiourea (PTU)-treated embryo media, and anesthetized with Tricaine for imaging at 4X magnification. MO efficiency was determined by extracting total RNA from embryos with Trizol (Invitrogen) according to manufacturer's instructions. Oligo-dT-primed total RNA was reverse transcribed using SuperScriptIII reverse transcriptase (Invitrogen) and cDNA was subsequently PCR amplified and sequenced using standard procedures.

Yeast two-hybrid screen

We carried out the yeast two-hybrid (Y2H) analysis using the Matchmaker Gal4-two hybrid system (Clontech), according to manufacturer's instructions. We amplified the full-length cDNA of mouse $Rpgr^{ORF15}$ or its different domains and cloned into the bait vector pGBKT7. The adult human retinal cDNA library was cloned into the ‘prey’ pGADT7 vector (Clontech) and used for the screen. Known-bait and known-prey analysis was carried out as described29.

Antibodies

Characterization of the $ORF15^{CP}$ antibody has been described24. Anti-RPGRIP1L antibody was generated by immunizing rabbits with the human

peptide ^{1300}HALQSVYKQYRDDLE^{1314} (Yenzym). RPGRIP1 antibody was a gift from Dr. Tiansen Li (Harvard Medical School); Antibodies against Xpress-tag and acetylated α-tubulin were procured from Invitrogen and Chemicon, respectively.

Mammalian cell culture, transient transfection, co-immunoprecipitation (coIP) and immunolocalization

We propagated COS-1 cells in DMEM plus 10%FBS, supplemented with Penicillin, Streptomycin and L-Glutamine. Co-IP experiments from retina and transfected cells have been described24. Immunolocalization studies in cells and in the retinal sections were carried out as reported previously4,30.

Supplementary Material

Refer to Web version on PubMed Central for supplementary material.

Acknowledgments

We thank the ciliopathy patients and their families for their continued support and encouragement. We also thank Heleen Arts for critical evaluation of the manuscript. This work was supported by grants R01EY007961 from the National Eye Institute (HK and AS), R01HD04260 from the National Institute of Child Health and Development (NK), R01DK072301, R01DK075972 (NK) R01DK068306, R01DK064614, R01DK069274 (FH), NRSA fellowship F32 DK079541 (EED) from the National Institute of Diabetes, Digestive and Kidney disorders, Intramural program of NEI (AS) the Macular Vision Research Foundation (NK), the Foundation for Fighting Blindness (HK, SSB, AS, and NK), the Foundation for Fighting Blindness Canada (RKK), Le Fonds de la recherche en sante du Québec (FRSQ) (RKK), Research to Prevent Blindness (AS), Harold Falls Collegiate Professorship (AS), the Midwest Eye Banks and Transplantation Center (HK), the Searle Scholars Program (MAB), the UK Medical Research Council (grant number G0700073; CAJ), NIHR Biomedical Research Centre for Ophthalmology (SSB) and EU-GENORET Grant LSHG-CT-2005-512036 (SSB). FH is an investigator of the Howard Hughes Medical Institute (HHMI) and a Doris Duke Distinguished Clinical Scientist (DDCF).

References

1. Badano JL, Mitsuma N, Beales PL, Katsanis N. The ciliopathies: an emerging class of human genetic disorders. Annu Rev Genomics Hum Genet. 2006; 7:125–48. [PubMed: 16722803]
2. Bergmann C, et al. Loss of nephrocystin-3 function can cause embryonic lethality, Meckel-Gruber-like syndrome, situs inversus, and renal-hepatic-pancreatic dysplasia. Am J Hum Genet. 2008; 82:959–70. [PubMed: 18371931]
3. Olbrich H, et al. Mutations in a novel gene, NPHP3, cause adolescent nephronophthisis, tapeto-retinal degeneration and hepatic fibrosis. Nat Genet. 2003; 34:455–9. [PubMed: 12872122]
4. Chang B, et al. In-frame deletion in a novel centrosomal/ciliary protein CEP290/NPHP6 perturbs its interaction with RPGR and results in early-onset retinal degeneration in the rd16 mouse. Hum Mol Genet. 2006; 15:1847–57. [PubMed: 16632484]
5. den Hollander AI, et al. Mutations in the CEP290 (NPHP6) gene are a frequent cause of Leber congenital amaurosis. Am J Hum Genet. 2006; 79:556–61. [PubMed: 16909394]
6. Baala L, et al. Pleiotropic effects of CEP290 (NPHP6) mutations extend to Meckel syndrome. Am J Hum Genet. 2007; 81:170–9. [PubMed: 17564974]
7. Leitch CC, et al. Hypomorphic mutations in syndromic encephalocele genes are associated with Bardet-Biedl syndrome. Nat Genet. 2008; 40:443–8. [PubMed: 18327255]
8. Sayer JA, et al. The centrosomal protein nephrocystin-6 is mutated in Joubert syndrome and activates transcription factor ATF4. Nat Genet. 2006; 38:674–81. [PubMed: 16682973]
9. Valente EM, et al. Mutations in CEP290, which encodes a centrosomal protein, cause pleiotropic forms of Joubert syndrome. Nat Genet. 2006; 38:623–5. [PubMed: 16682970]

10. Badano JL, et al. Dissection of epistasis in oligogenic Bardet-Biedl syndrome. Nature. 2006; 439:326–30. [PubMed: 16327777]
11. Tory K, et al. High NPHP1 and NPHP6 mutation rate in patients with Joubert syndrome and nephronophthisis: potential epistatic effect of NPHP6 and AHI1 mutations in patients with NPHP1 mutations. J Am Soc Nephrol. 2007; 18:1566–75. [PubMed: 17409309]
12. Gherman A, Davis EE, Katsanis N. The ciliary proteome database: an integrated community resource for the genetic and functional dissection of cilia. Nat Genet. 2006; 38:961–2. [PubMed: 16940995]
13. Liu Q, et al. The proteome of the mouse photoreceptor sensory cilium complex. Mol Cell Proteomics. 2007; 6:1299–317. [PubMed: 17494944]
14. Arts HH, et al. Mutations in the gene encoding the basal body protein RPGRIP1L, a nephrocystin-4 interactor, cause Joubert syndrome. Nat Genet. 2007; 39:882–8. [PubMed: 17558407]
15. Delous M, et al. The ciliary gene RPGRIP1L is mutated in cerebello-oculo-renal syndrome (Joubert syndrome type B) and Meckel syndrome. Nat Genet. 2007; 39:875–81. [PubMed: 17558409]
16. Gerdes JM, et al. Disruption of the basal body compromises proteasomal function and perturbs intracellular Wnt response. Nat Genet. 2007; 39:1350–60. [PubMed: 17906624]
17. Ross AJ, et al. Disruption of Bardet-Biedl syndrome ciliary proteins perturbs planar cell polarity in vertebrates. Nat Genet. 2005; 37:1135–40. [PubMed: 16170314]
18. Corbit KC, et al. Kif3a constrains beta-catenin-dependent Wnt signalling through dual ciliary and non-ciliary mechanisms. Nat Cell Biol. 2008; 10:70–6. [PubMed: 18084282]
19. Beales PL, et al. IFT80, which encodes a conserved intraflagellar transport protein, is mutated in Jeune asphyxiating thoracic dystrophy. Nat Genet. 2007; 39:727–9. [PubMed: 17468754]
20. Otto EA, et al. Nephrocystin-5, a ciliary IQ domain protein, is mutated in Senior-Loken syndrome and interacts with RPGR and calmodulin. Nat Genet. 2005; 37:282–8. [PubMed: 15723066]
21. Shu X, et al. RPGR mutation analysis and disease: an update. Hum Mutat. 2007; 28:322–8. [PubMed: 17195164]
22. Breuer DK, et al. A comprehensive mutation analysis of RP2 and RPGR in a North American cohort of families with X-linked retinitis pigmentosa. Am J Hum Genet. 2002; 70:1545–54. [PubMed: 11992260]
23. Hong DH, et al. RPGR isoforms in photoreceptor connecting cilia and the transitional zone of motile cilia. Invest Ophthalmol Vis Sci. 2003; 44:2413–21. [PubMed: 12766038]
24. Khanna H, et al. RPGR-ORF15, which is mutated in retinitis pigmentosa, associates with SMC1, SMC3, and microtubule transport proteins. J Biol Chem. 2005; 280:33580–7. [PubMed: 16043481]
25. Oprea GE, et al. Plastin 3 is a protective modifier of autosomal recessive spinal muscular atrophy. Science. 2008; 320:524–7. [PubMed: 18440926]
26. Giess R, et al. Early onset of severe familial amyotrophic lateral sclerosis with a SOD-1 mutation: potential impact of CNTF as a candidate modifier gene. Am J Hum Genet. 2002; 70:1277–86. [PubMed: 11951178]
27. Badano JL, Katsanis N. Beyond Mendel: an evolving view of human genetic disease transmission. Nat Rev Genet. 2002; 3:779–89. [PubMed: 12360236]
28. Dryja TP, et al. Null RPGRIP1 alleles in patients with Leber congenital amaurosis. Am J Hum Genet. 2001; 68:1295–8. [PubMed: 11283794]
29. Cheng H, et al. Photoreceptor-specific nuclear receptor NR2E3 functions as a transcriptional activator in rod photoreceptors. Hum Mol Genet. 2004; 13:1563–75. [PubMed: 15190009]
30. He S, et al. Retinitis Pigmentosa GTPase Regulator (RPGR) protein isoforms in mammalian retina: insights into X-linked Retinitis Pigmentosa and associated ciliopathies. Vision Res. 2008; 48:366–76. [PubMed: 17904189]

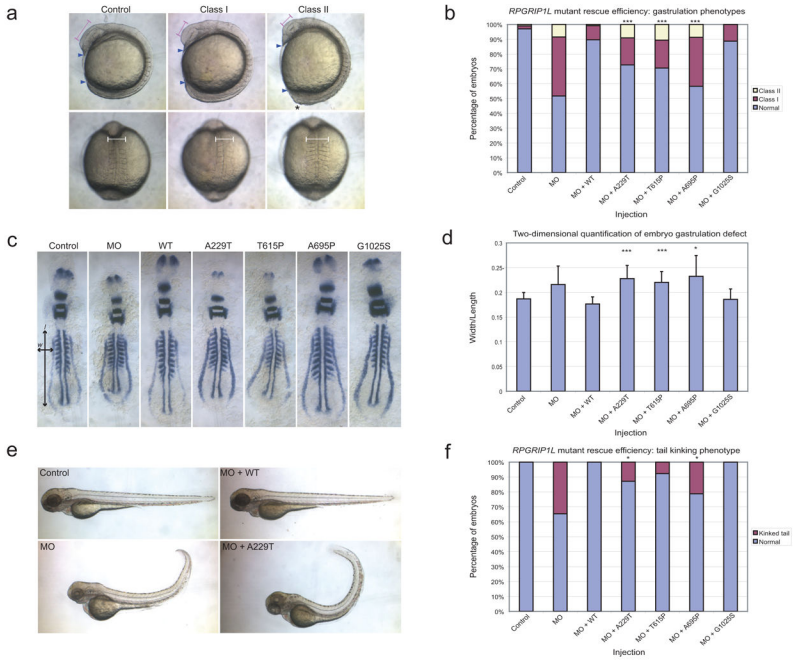

Figure 1. Functional assessment of the *RPGRIP1L* A229T variant *in vivo*

a. Zebrafish embryos injected with *rpgrip1l* splice-blocking morpholino (MO) display gastrulation defects at the eight-nine somite stage; lateral and dorsal views of live embryos are shown. Embryos were categorized phenotypically based on the presence of a shortened body axis (anterior and posterior ends indicated with blue triangles) and small head/eyes only (magenta lines indicate eye size) (Class I; mild); or shortened body axis and small head/eyes in addition to at least one of the following: broad and thin somites (white line indicates somite span), notochord kinking, and tail extension defects (black asterisk) (Class II; severe).

b. Live scoring of embryos co-injected with MO and human *RPGRIP1L* mRNA indicates that A229T is pathogenic in our assay as indicated by the comparison of WT rescue efficiency to mutant rescue efficiency. MO, morpholino alone; WT, wild-type human *RPGRIP1L* mRNA. Known JBTS mutations T615P and A695P are positive controls; neutral variant G1025S (rs2111119) is a negative control. Statistical significance (mutant rescue vs. WT rescue) is depicted as (***), $p<0.0001$ (χ^2); see Suppl Table 2 for all χ^2 and p-values.

c. Representative examples of whole-mount embryos hybridized *in situ* with *pax2*, *krox20*, and *myoD* riboprobes.

d. Two-dimensional morphometric quantification of the efficiency of human *RPGRIP1L* mRNA to rescue *rpgrip1l* MO phenotypes. Whole embryos with eight-nine appreciable somites (n=8-20/injection) labeled with *pax2*, *krox20*, and *myoD* riboprobes were flat-mounted, photographed and measured in two dimensions. The width/length ratio was calculated as the width (w) spanning between the distal ends of the 5th anterior somites (horizontal arrow in panel **c**) vs. the length (l) of the notochord as indicated by the staining of adaxial cells (vertical arrow in panel **c**). Statistical significance (mutant vs. WT rescue) is depicted as (*), $p<0.05$ and (***), $p<0.0001$ (two-tailed student's t-test); see Suppl Table 3 for all p-values.

e. *rpgrip1l* morphant larvae display tail development defects at 5 days post-fertilization (dpf). Morphant larva (MO) with tail curvature and posterior structural disorganization can be rescued efficiently with WT human *RPGRIP1L* mRNA, however *RPGRIP1L* message harboring the 229T encoding allele does not completely rescue the tail phenotype.
f. Quantification of the efficiency of tail phenotype rescue in 5dpf larvae. Whereas WT *RPGRIP1L* message completely rescued the tail phenotypes, A229T as well as positive controls T615P and A695P result in the persistence of affected tail structures in injected larva. G1025S was used as a negative control. Statistical significance (mutant rescue vs. WT rescue) is depicted as (*), $p<0.05$ (χ^2).

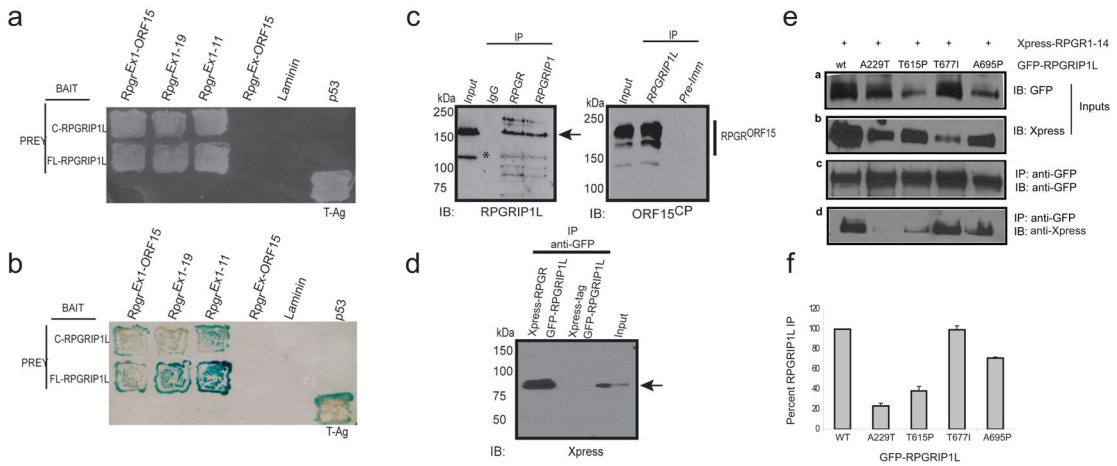

Figure 2. RPGRIP1L interacts with RPGR and missense variant A229T abrogates this interaction

a. Known-bait and known-prey analysis. Yeast two-hybrid analysis using indicated RPGR bait-encoding constructs and RPGRIP1L [carboxyl-terminal (C) or full-length (FL)] prey encoding constructs revealed interaction of RPGR exons 1-11 with carboxyl-terminal or full-length RPGRIP1L. Laminin was used as negative control, whereas p53/T-antigen (T-Ag) interaction served as a positive control.

b. RPGR-RPGRIP1L interaction was validated further by examining the activation of the *LacZ* gene in the β-galactosidase assay corresponding to (**a**).

c. Interaction of RPGR and RPGRIP1L *in vivo*. Bovine retinal extracts were subjected to immunoprecipitation (IP) using anti-RPGR, RPGRIP1, RPGRIP1L antibodies, normal immunoglobulin (IgG), or pre-immune serum (Pre-Imm). Precipitated proteins were analyzed by SDS-PAGE and immunoblotting (IB) using anti-RPGRIP1L (left) or RPGR-ORF15^{CP} antibody (right). Arrow (left) indicates RPGRIP1L-imunoreactive band and the straight line in the right panel depicts the RPGR isoforms pulled down by RPGRIP1L. Asterisk (*) marks a non-specific immunoreactive band.

d. RPGR-RPGRIP1L interaction in transfected cells. COS-1 cells were transiently transfected with constructs encoding Xpress-tagged RPGR, GFP-RPGRIP1L or Xpress-tag alone. Proteins were extracted and subjected to immunoprecipitation (IP) using the anti-GFP antibody. Precipitated proteins were analyzed by SDS-PAGE and immunoblotting using anti-Xpress antibody. Input lane contains 20% of the protein extract used for IP. Arrow indicates the Xpress-immunoreactive band.

e. Interaction of RPGR with wild-type (WT) and mutant RPGRIP1L. COS-1 cells were transiently transfected with constructs encoding WT or mutant RPGRIP1L fused to GFP and Xpress-tagged RPGR. Panels ‘a’ and ‘b’ indicate the 20% of the GFP-RPGRIP1L and Xpress-RPGR input protein extract used for IP. Precipitation of GFP-RPGRIP1L using the GFP antibody was used as a positive control (panel ‘c’). Association of wt and mutant GFP-RPGRIP1L with Xpress-RPGR is represented in Panel ‘d’. T677I represents a *bona fide* pathogenic allele, but which likely does not contribute to retinal degeneration.

f. Quantitative analysis of the band intensities are represented as percent of mutant RPGRIP1L immunoprecipitated by RPGR. Association of wt GFP-RPGRIP1L with RPGR was considered as 100%. The results represent an average of three independent experiments.

Table 1

Total mutational load in northern European ciliopathy patients with *RPGRIP1L* variants

Clinical Diagnosis	Patient ID	*RPGRIP1L* Alleles		Allele Frequency in Controls	Other Alleles
LCA	3184	S199G		0/192	
LCA	340	A229T		84/3016	*RPGR:* I1148V het
LCA	341	A229T	A229T	84/3016	*LCA5:* Q279X het
LCA	1972	L546F		0/192	
LCA	1321	V647I		0/192	*CRB1:* C948Y hom
LCA	1378	T677I		0/260	*RPGRIP:* R890X hom
LCA	1380	T677I		0/260	
LCA	1617	R937L		0/192	
LCA	3182	A1183G		4/192	*RPGR:* I1148V het
LCA	3189	A1183G		4/192	*RPGR:* I1148V het, N1081K het
LCA	3181	D1264Y		0/192	*RPGR:* I1148V het
LCA	3187	D1264Y		0/192	*RPGR:* I1148V het
LCA	3192	D1264Y		0/192	
SLS	F259-II1	A229T		84/3016	*NPHP5:* R364X het
SLS	F848-II1	A229T		84/3016	*NPHP5:* T627M het, *CEP290:* R1978X het
SLS	F99-II1	A229T		84/3016	*NPHP3:* R397H het, S500P het
JBTS	F256-II1	A229T		84/3016	*CEP290:* Q1591X het
BBS	AR74-05	A229T		84/3016	
BBS	AR400-03	A229T		84/3016	
BBS	AR672-03	A229T		84/3016	
BBS	AR775-03	A229T		84/3016	*MKS1:* D286G het
BBS	AR348-03	L447S		0/192	
BBS	AR623-03	A1183G		4/192	
MKS	MKS-060143	R1236C		0/192	

Table 2

Frequency of *RPGRIP1L* A229T (c.685G>A; rs61747071) in ciliopathy patients of northern European descent

Clinical Diagnosis	n=	Genotype Counts			Genotype Frequency			Allele Counts		Allele Frequency		p-values			
												Cases v. Controls[1]	RP v. Non-RP[1]	Cases v. Controls[2]	RP v. Non-RP[2]
		GG	GA	AA	GG	GA	AA	G	A	G	A				
Controls	1508	1425	82	1	0.945	0.054	0.001	2932	84	0.972	0.028				
NPHP	66	66	0	0	1	0	0	132	0	1	0				
MKS	49	49	0	0	1	0	0	98	0	1	0				
Ciliopathy Non-RP	**115**	**115**	**0**	**0**	1	0	0	**230**	**0**	1	0	**1.92E-03**		**1.54E-03**	
LCA	189	174	14	1	0.921	0.074	0.005	362	16	0.958	0.042				
SLS	84	75	9	0	0.893	0.107	0	159	9	0.946	0.054				
JBTS	30	25	5	0	0.833	0.167	0	55	5	0.917	0.083				
BBS	184	170	14	0	0.924	0.076	0	354	14	0.962	0.038				
Ciliopathy RP	**487**	**444**	**42**	**1**	0.912	0.086	0.002	**930**	**44**	0.955	0.045	**6.45E-03**	**7.35E-05**	**0.021**	**1.66E-05**

[1] Fisher's exact test, 1-tailed; 2-tailed p-values remained significant (Ciliopathy Non-RP v. Controls, p=3.84E-03; Ciliopathy RP v. Controls, p=0.013; Ciliopathy Non-RP v. Ciliopathy RP, p=1.47E-04)

[2] Permutation test

Table 3

Functional assessment of *RPGRIP1L* missense variants in an *in vivo* zebrafish model

		Conservation	*In vivo* modeling in zebrafish	
Variant	**Domains***	**Species****	**Live scoring**	**Quantitative**
S199G	CCI	*Ptr, Bta, Cfa, Mmu, Oan, Dre*	pathogenic	pathogenic
A229T	CCI	*Ptr, Mmul, Eca, Bta, Cfa, Rno, Mmu, Mdo, Dre*	pathogenic	pathogenic
L447S	CCIV	*Ptr, Mmul*	benign	benign
L546F	CCV	*Ptr, Mmul, Eca, Bta, Cfa, Rno, Mmu, Mdo, Oan, Gga, Dre*	pathogenic	pathogenic
T615P	C2	*Ptr, Mmul, Eca, Bta, Cfa, Mmu, Mdo*	pathogenic	pathogenic
V647I	C2	*Ptr, Mmul, Mdo, Oan, Gga, Dre, Spu*	pathogenic	benign
T677I	C2	*Ptr, Mmul, Eca, Bta, Cfa, Rno, Mmu, Oan*	pathogenic	pathogenic
A695P	C2	*Ptr, Mmul, Eca, Bta, Cfa, Rno, Mmu, Mdo, Oan, Dre, Spu*	pathogenic	pathogenic
R937L		*Ptr, Mmul, Cfa*	pathogenic	pathogenic
A1183G	RID	*Ptr, Mmul, Eca, Bta, Cfa, Rno, Mmu, Mdo, Oan, Gga*	pathogenic	pathogenic
R1236C	RID	*Ptr, Mmul, Eca, Bta, Cfa, Rno, Mmu, Mdo, Oan, Spu*	pathogenic	pathogenic
D1264Y	RID	*Eca, Bta, Cfa, Rno, Mmu*	pathogenic	pathogenic

* CC- Coiled coil domain; C2- protein kinase C (PKC) conserved region 2 motif; RID- domain with homology to the RPGR-interacting domain of RPGRIP1.

** Ptr- Pan troglodytes; Mmul- M. mulatta; Eca- E. caballus; Bta- B. taurus; Cfa- C. familiaris; Rno- R. norvegicus; Mmu- M. musculus; Mdo- M. domestica; Oan- O. anatinus; Gga- G. gallus; Dre- D. rerio; Spu- S. purpuratus